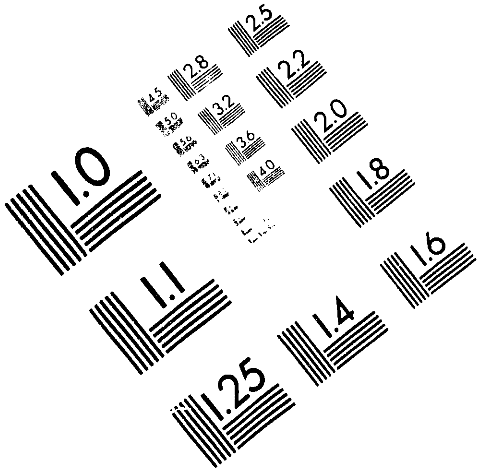

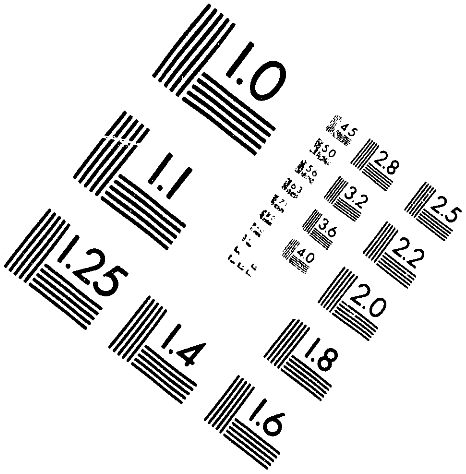

AIIM

Association for Information and Image Management

1100 Wayne Avenue, Suite 1100
Silver Spring, Maryland 20910
301/587-8202

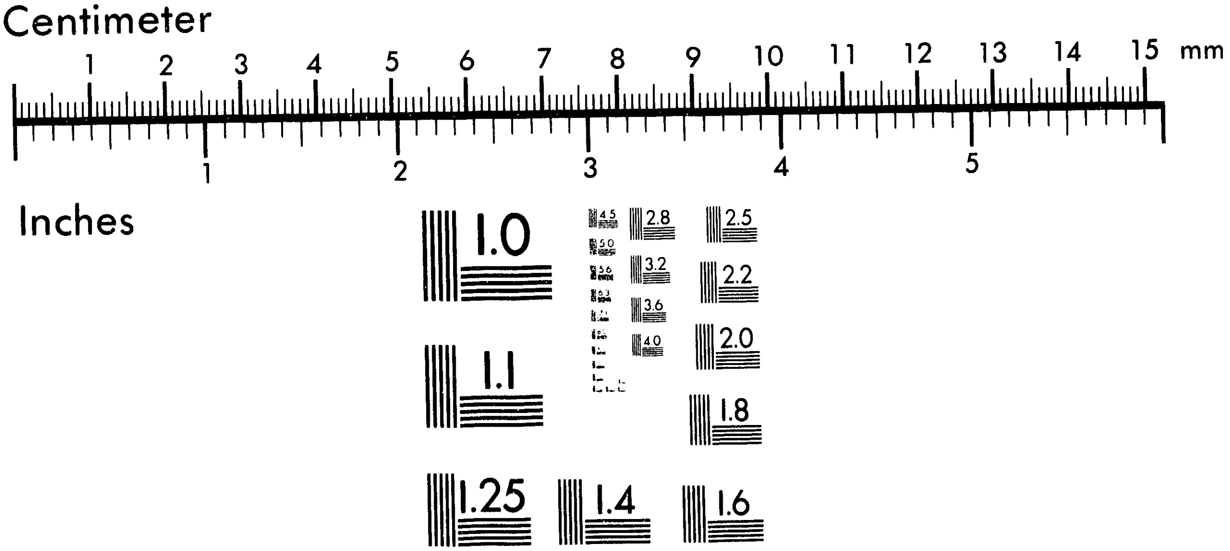

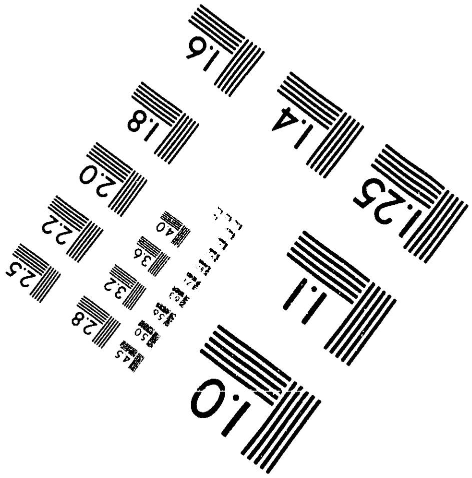

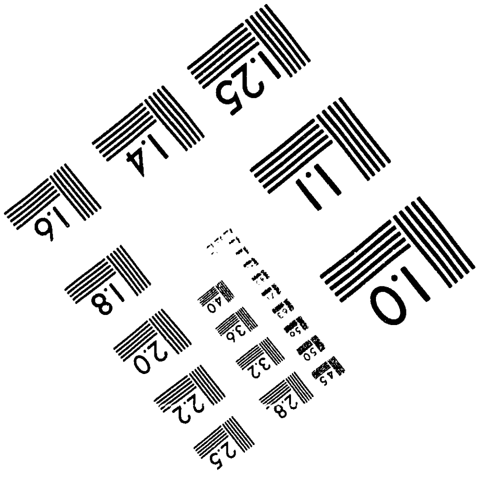

MANUFACTURED TO AIIM STANDARDS
BY APPLIED IMAGE, INC.

1 of 1

2

Conf-930405--23

RECEIVED
JUN 21 1993
OSTI

PNL-SA-21667

CHARACTERIZATION OF NANOSCALE OXIDE AND OXYHYDROXIDE POWDERS USING EXAFS SPECTROSCOPY

J. G. Darab
Y. Ma
J. C. Linehan
D. W. Matson

June 1993

Presented at the
Material Research Society
Spring 1993 Meeting
April 12-16, 1993
San Francisco, California

Prepared for
the U.S. Department of Energy
Contract DE-AC06-76RLO 1830

Pacific Northwest Laboratory
Richland, Washington 99352

CHARACTERIZATION OF NANOSCALE OXIDE AND OXYHYDROXIDE POWDERS USING EXAFS SPECTROSCOPY

JOHN G. DARAB*, J. C. LINEHAN*, Y. MA** AND D. W. MATSON*
*Pacific Northwest Laboratory[1], P.O. Box 999, Richland, WA 99352
**Physics Department, University of Washington, Seattle, WA 98195

ABSTRACT

Extended x-ray absorption fine structure (EXAFS) spectroscopy has been used to determine the structural environment local to iron(III) and zirconium(IV) cations in respectively, nanoscale iron oxyhydroxide and nanoscale zirconium oxide powders. The iron oxyhydroxide powder, produced by the modified reverse micelle (MRM) technology, was found to have a short-range structure most similar to that of goethite (α-FeOOH). The short-range structure of the zirconium oxide powder, produced using the rapid thermal decomposition of solutes (RTDS) technology, was found to be a mixture of monoclinic zirconia and cubic zirconia environments.

INTRODUCTION

Metal oxide and oxyhydroxide powders with nanometer-sized grains are useful in a variety of industrial applications as catalysts and as precursors for advanced structural and magnetic materials. Tens-of-gram quantities of a variety of pure and alloyed metal and oxide nanoscale powders have been produced using the modified reverse micelle (MRM) and rapid thermal decomposition of solute (RTDS) technologies developed at Pacific Northwest Laboratory.

MRMs are thermodynamically stable water-in-oil microemulsions in which the 1-20 nanometer sized aqueous cores are stabilized in the presence of high (1.0 M) metal salts by appropriate combinations of surfactants [2]. Nanoscale particle formation is accomplished by polymerizing or reducing the metal complexes formed in the confining aqueous phase by adding to the microemulsion another MRM containing a strong base or a reducing agent.

In the RTDS process, an aqueous solution (0.1-0.5 M) containing dissolved thermally labile metal precursor salt(s) are passed through a short section of heated tubing at high pressures and flow rates before expanding through a nozzle. Nanoscale metal oxyhydroxide particle formation is initiated as the solution is heated and abruptly stops at the point of expansion.

The relationship between processing, structure, and properties becomes critical when dealing with nanoscale materials. Traditional x-ray diffraction (XRD) techniques applied to nanoscale powders have yielded little structural information. Here we discuss the use of extended x-ray absorption fine structure (EXAFS) spectroscopy in the structural elucidation of two specific powder systems: an MRM iron oxyhydroxide and an RTDS zirconium oxide.

The details of producing the MRM [2] and RTDS [3] powders have been described elsewhere. Table I summarizes some of the characteristics of the as-prepared MRM iron oxyhydroxide and RTDS zirconium oxide powders studied in this work. Note the level of carbon and sulfur impurities in the MRM powder, which is consistent with sulfate surfactant incorporation. The particle morphology of a typical RTDS zirconium oxide nanoscale powder is illustrated in Figure 1.

Table I. Summary of attributes of the MRM iron oxyhydroxide and the RTDS zirconium oxide nanoscale powders.

powder	iron oxyhydroxide	zirconium oxide
production method	MRM	RTDS
phases detected[a]	2-line ferrihydrite	cubic zirconia
average grain size	<10-nm[a,b]	<10-nm[a,b]
average agglomerate size	5000-nm[c]	50-nm[b]
elemental analysis[d]:		
C	11.62-wt%	1.23-wt%
H	2.98	0.68
N	0.12	0.70
Na	0.17	-
S	2.56	-
Determined by [a]XRD, [b]TEM, [c]SEM, [d]independent laboratory analysis.		

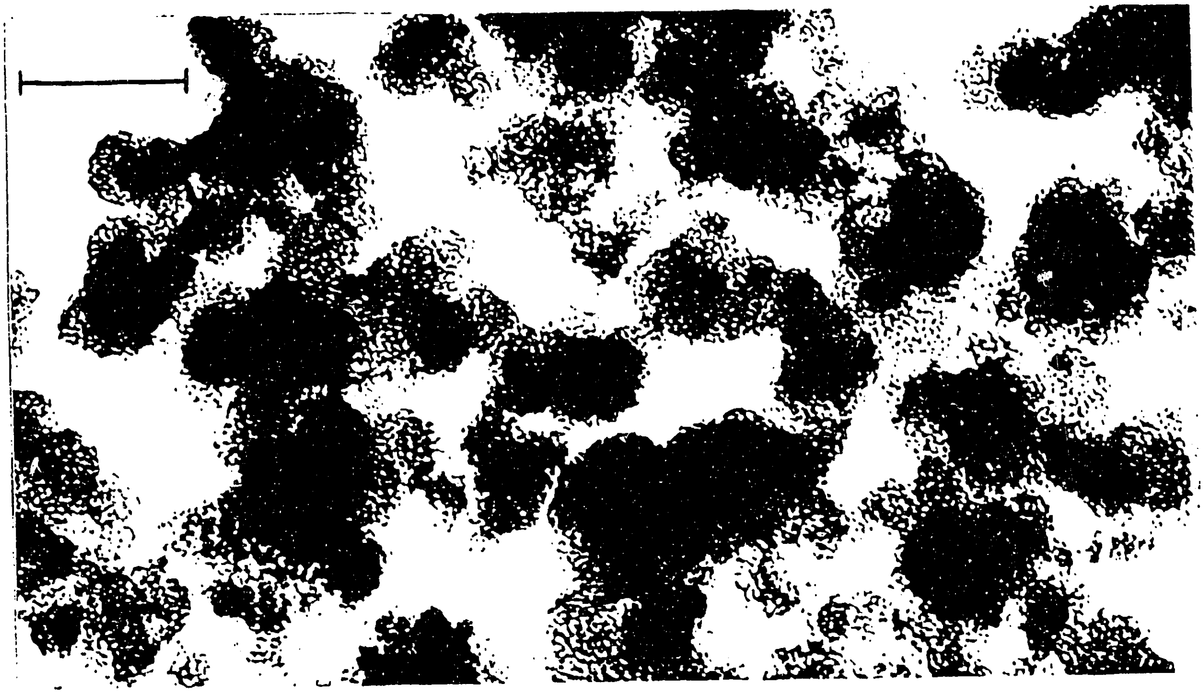

Figure 1. Bright field transmission electron micrograph of a typical RTDS zirconium oxide nanoscale powder. Bar equals 50-nm.

EXPERIMENTAL

EXAFS Standards

Hematite (α-Fe_2O_3), maghemite (γ-Fe_2O_3), magnetite (Fe_3O_4), goethite (α-FeOOH), akaganeite (β-FeOOH), feroxyhyte (δ'-FeOOH), lepidocrocite (γ-FeOOH), ferric oxyhydroxysulfate ($Fe_8O_8(OH)_6SO_4$), six-line ferrihydrite ($5Fe_2O_3 \cdot 9H_2O$), and two-line ferrihydrite (unknown structural formula) standards were prepared by the well-established procedures detailed by Schwertmann and Cornell [4]. Phase purity in each case was confirmed by x-ray diffraction (XRD) and Mossbauer spectroscopy.

Monoclinic zirconia (m-ZrO_2) and cubic 8-wt% yttria-zirconia (c-ZrO_2) were obtained from commercial sources. Phase purity was confirmed in both cases by XRD.

EXAFS Analysis

Iron and zirconium K-edge EXAFS spectra were obtained at room temperature on beam line X19A at the National Synchrotron Light Source. The data were obtained in a transmission mode using the as-prepared powders thinly distributed onto cellophane tape. The beam line used a Si(220) double crystal monochromator and standard ionization detectors. The beam was detuned 50-60% to reduce the content of higher harmonics. The incident and transmitted x-ray intensities were recorded as a function of x-ray energy, E, allowing the absorption coefficient, $\mu(E)$, to be determined.

Standard EXAFS data analysis were applied to the averaged data [5]. The $\chi(E)$ data were obtained from $\mu(E)$ by the usual method of normalization and subtraction of the smoothly varying background, $\mu_0(E)$. The data were then converted to $\chi(k)$ using the onset of the absorption edge as the energy origin, E_0. The $\chi(k)$ data were then Fourier transformed to real space over appropriate k-ranges yielding radial structure plots (RSPs). From RSPs obtained by Fourier transforming over 2.5-11.5 Å^{-1}, which emphasizes the contributions of the lighter nuclei scatterers, the first-neighbor feature of each RSP was then back-Fourier transformed to obtain the respective $\chi(k)$ envelopes. Second-neighbor $\chi(k)$ envelopes were similarly determined from RSPs obtained by Fourier transforming the same data over 5.7-11.5 Å^{-1}, which emphasizes the contributions of the heavier nuclei scatterers.

RESULTS AND DISCUSSION

The relation which describes the EXAFS phenomenon is generally expressed as

$$\chi(k) = [-N/(kR^2)]\, f(k) \sin[2kR + \phi(k)] \exp[-2k^2\sigma^2] \exp[-2R/\lambda(k)] \qquad (1)$$

where N is the number of backscatterers in a particular nearest neighbor shell surrounding the atom of interest, R is the average radius of the nearest neighbor shell, f(k) is the backscattering amplitude, $\phi(k)$ is the total phase shift experienced by the photoelectron upon being scattered, σ^2 is the mean square vibrational displacement of the scatterers, and $\lambda(k)$ is the mean free path of the scattered photoelectron [5].

Using the $\chi(k)$ envelope of a particular neighbor shell obtained from a standard or a group of standards with known values of N, R and σ as a basis, the $\chi(k)$ envelope of the same neighbor shell obtained from an unknown material can be fitted by systematically varying N, R and σ in expression (1) using a single set or linear combination of variables involving one or several standards. This technique is valid as long as the structure and chemistry of the unknown material is similar to (i.e., transferable with) that of the standards. In this work, the structural and chemical transferability between an unknown material and a standard is verified by demonstrating that the difference in ϕ at k equals zero between the unknown and the standard is equal to zero [5].

MRM Iron Oxyhydroxide Nanoscale Powder

Of all the standards investigated, only the two-line ferrihydrite, goethite and ferric oxyhydroxysulfate standards proved to be structurally and chemically transferable with those of the MRM iron oxyhydroxide powder for both the first and second neighbor shells. The results of the least squares fitting of the $\chi(k)$ envelopes obtained from the MRM iron oxyhydroxide powder using the two-line ferrihydrite, goethite and ferric oxyhydroxysulfate standards are summarized in Table II. The best fit, illustrated in Figure 2, was obtained using the goethite standard as a basis for fitting $\chi(k)$. Least squares fitting using linear combinations of several standards did not produce as good of a fit as that obtained from goethite alone.

Table II. Results of least squares fitting of the $\chi(k)$ envelopes obtained from the MRM iron oxyhydroxide powder.

	first neighbor shell		second neighbor shell	
standard	$R - R_{std}$ (Å)	N/N_{std}	$R - R_{std}$ (Å)	N/N_{std}
two-line ferrihydrite	-0.02	1.41	-0.02	0.27
goethite	-0.02	0.99	-0.00	0.35
ferric oxyhydroxysulfate	-0.02	1.39	-0.01	0.52

For the two-line ferrihydrite, goethite and ferric oxyhydroxysulfate phases studied here, the first neighbor shell corresponds to oxygen in the aquo, hydroxy and oxy ligands, ~~which~~ STET form predominantly octahedral complexes with the iron(III) cation. The second neighbor shell corresponds to predominantly iron(III) cations in adjacent edge sharing octahedra [4]. Table II indicates that within experimental error (at least ±0.02-Å), the nearest neighbor radii of the MRM iron oxyhydroxide powder are identical to those of two-line ferrihydrite, goethite and ferric oxyhydroxysulfate.

In addition, considering that the best fit to the experimental $\chi(k)$ data was obtained using goethite as a standard and that the number of first nearest neighbors agrees extremely well with that which is expected for goethite, it ~~becomes suggestive~~ appears that the MRM iron oxyhydroxide nanoscale powder has a short-range structure ~~which~~ that is most similar to that of goethite.

One reason for the much smaller number of second nearest neighbors in the MRM iron oxyhydroxide compared to that of goethite is the nanometer size grains of the MRM powder. However, the lack of any longer range order (via XRD) indicative of small goethite crystallites suggests that the MRM powder is a disordered form of goethite, which we have defined as proto-goethite [2]. The disorder is most likely due to the incorporation of sulfates into the material [5].

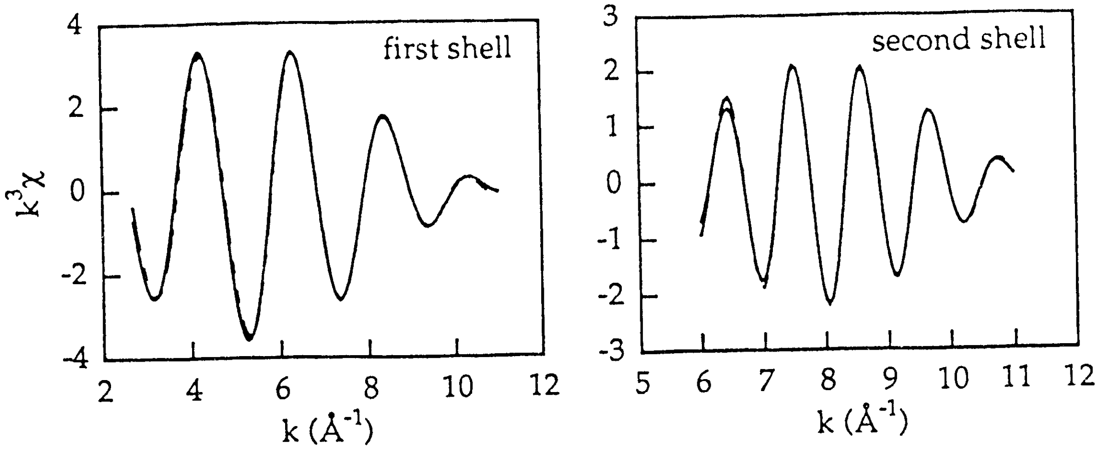

Figure 2. Least squares fitting (solid lines) of the $\chi(k)$ envelopes obtained from the MRM iron oxyhydroxide powder (dashed lines) using goethite as a standard. Notice that the experimental and fitted curves are nearly indistinguishable.

RTDS Zirconium Oxide Nanoscale Powder

For the case of the as-prepared RTDS zirconium oxide powder, the situation is more complex. The results of the least squares fitting of the $\chi(k)$ envelopes obtained from the RTDS zirconium oxide powder using linear combinations of the monoclinic and cubic zirconia standards are summarized in Table III. The fit to the first and second neighbor shells using linear combinations of both standards are illustrated in Figure 3. Much poorer fits were obtained when only a single standard was used.

Table III. Results of least squares fitting of the $\chi(k)$ envelopes obtained from the RTDS zirconium oxide powder using linear combinations of the c-ZrO_2 and m-ZrO_2 standards.

first neighbor shell			second neighbor shell		
components	R - R_{std} (Å)	N/N_{std}	components	R - R_{std} (Å)	N/N_{std}
76% c-ZrO_2	+0.01	1.00	35% c-ZrO_2	-0.15	0.79
24% m-ZrO_2	-0.02	1.00	65% m-ZrO_2	-0.13	0.79

For the family of zirconium oxide phases investigated here, the first neighbor shell corresponds to oxygen in the oxy ligands which form predominantly seven (m-ZrO_2) and eight (c-ZrO_2) coordinate complexes with the zirconium(IV) cation. The second neighbor shell corresponds to predominantly zirconium(IV) cations in corner sharing polyhedra [6]. The excellent fit to the experimental first neighbor $\chi(k)$ envelope using linear combinations of monoclinic and cubic zirconia standards and the close agreement in first neighbor radii strongly indicates that the average short-range structure of the RTDS zirconium oxide nanoscale powder is a combination of both these phases.

The contribution of the c-ZrO_2 standard in the fitting of the first neighbor $\chi(k)$ data is corroborated by the XRD results. However, the fact that the structure of the

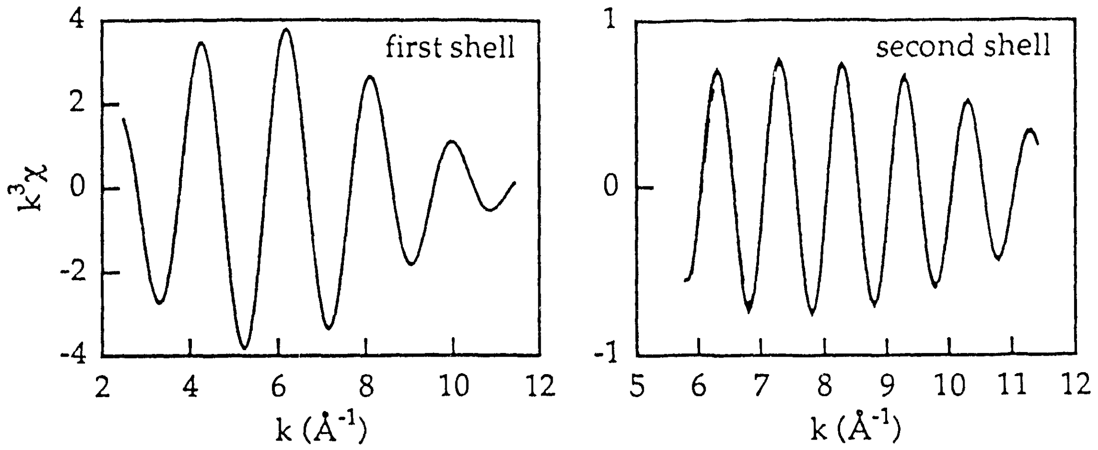

Figure 3. Least squares fitting (solid lines) of the $\chi(k)$ envelopes obtained from the RTDS zirconium oxide powder (dashed lines) using c-ZrO_2 and m-ZrO_2. Notice that the experimental and fitted curves are nearly indistinguishable.

first neighbor shell of the RTDS zirconium oxide nanoscale powder is predominantly similar to c-ZrO_2 with nearly identical bond lengths, whereas that of the second neighbor shell has significantly different bond lengths than both standards is not revealed by traditional XRD techniques. This effect is most likely due to disorder associated with the nanometer size grains of the RTDS powder.

SUMMARY

EXAFS spectroscopy has been used to obtain structural information about the nanoscale MRM iron oxyhydroxide and nanoscale RTDS zirconium oxide powders. which could not be determined using XRD techniques. The MRM iron oxyhydroxide powder was found to have a structure most similar to that of a disordered form of goethite (α-FeOOH). The short-range structure of the RTDS zirconium oxide powder was found to be a mixture of monoclinic zirconia and cubic zirconia environments.

ACKNOWLEDGEMENTS

This work was supported by the U.S. Department of Energy, Office of Fossil Energy and by the Advanced Processing Technology Initiative at Pacific Northwest Laboratory.

REFERENCES

1. Pacific Northwest Laboratory is operated for the U.S. Department of Energy by the Battelle Memorial Institute under contract DE-AC06-76RLO 1830.
2. J.G. Darab, J.L. Fulton and J.C. Linehan in Preprints, Division of Fuel Chemistry (American Chemical Society, Washington, D.C., 1993) 38, 27.
3. D.W. Matson, J.C. Linehan and M.E. Geusic, *Part. Sci. Tech.* 10, 143 (1992).
4. U. Schwertmann and R.M. Cornell, Iron Oxides in the Laboratory (Weinheim, New York, 1991).
5. P.A. Lee, P.H. Citrin, P. Eisenberger and B.M. Kincaid, *Rev. Mod. Phys.* 53, 759 (1981).
6. R. Stevens, Zirconia and Zirconia Ceramics (Magnesium Elektron Ltd, Twickenham, UK, 1986).

DATE FILMED

8/23/93

END